Tellus (1994), 46A, 541–552
Printed in Belgium – all rights reserved

TELLUS
ISSN 0280–6495

An ENSO impact on Europe?

A review

By KLAUS FRAEDRICH, *Meteorologisches Institut, Universität Hamburg, D-20146 Hamburg, Germany*

(Manuscript received 11 August 1993; in final form 20 December 1993)

ABSTRACT

The possible influence of the El Niño/Southern Oscillation (ENSO) warm and cold extremes on mid-latitude circulation regimes in the North Atlantic/European sector is described in terms of a phenomenological, statistical and physical analysis of observational data. (1) The European circulation patterns (after Hess-Brezowsky, 1977) are combined to a binary set of cyclonic and anticyclonic (low and high pressure) centres of action. They reveal a regional ENSO response with predominantly cyclonic (anticyclonic) Grosswetter for warm (cold) ENSO events in winters at the peak of the episode. (2) Standard climate statistics of the same winter seasons (surface pressure, temperature and precipitation anomalies) supplement the Grosswetter phenomenology. They suggest a shift of the tail end of the cross Atlantic storm track and its rainbearing frontal systems from a more northern route (during warm events) to a more zonal orientation (in cold events). (3) Finally, the transient and stationary eddy-mean flow interaction is diagnosed from daily hemispheric 500 mb geopotential height fields. They are composited about most extreme anomalies in Europe (independent of ENSO) defined by the amplitude of the first simultaneous EOF of normalized monthly mean pressure, temperature and precipitation at 40 stations. Thus (upstream location and intensity of) dynamic sources of wave activity flux in the western North-Atlantic cyclogenesis area can be identified. They are associated with European climate anomalies and may represent the connection linking ENSO and Europe under favourable conditions.

1. Introduction

Detecting a statistically significant and physically meaningful response of the eastern North Atlantic/European sector on the El Niño/Southern Oscillation (ENSO) forcing in the equatorial Pacific, may have two important consequences. (a) The North Atlantic/European sector could be classified as an area with a potential for long-range weather forecasting, and (b) the analysis of the underlying physical mechanisms, feedbacks and interactions may challenge numerical experiments, physically directed diagnostic studies and conceptual model building. Therefore, the present study is aimed to provide some background for the analysis of a possible ENSO-Europe link. It should be noted that the emphasis of most diagnostic ENSO studies lies on the response in the nearby tropical regions or, in the mid-latitudes, on the impact in adjacent areas like the eastern North Pacific, North America and Australia. The possibility of an ENSO impact on European climate has only been of marginal interest until recently (see Palmer and Anderson, 1993). Before proceeding to a more detailed study of a possible European ENSO response, a brief summary of some of the relevant studies on short term climate predictability and ENSO affecting Europe is given.

Van Loon and Madden (1981, Figs. 3–7) analysed the global associations of ENSO correlating and compositing northern winter pressure and temperature fields. While the ENSO (warm–cold) induced difference over the eastern North Pacific reveals the Pacific-North America pattern (PNA) as a zonally oriented dipole (Aleutian Low and Canada High), the North

Atlantic response shows the north–south sea-saw or North Atlantic Oscillation (NAO, with Iceland Low and Azores High). In the European/North Atlantic sector they found significant correlations in the pressure and temperature fields over Scandinavia. Subdivision of their 80-year data set into four 20-year sets shows stability of the ENSO-Europe correlation in three of the subsets.

Hamilton (1988, Figs. 7, 20 and 21) evaluated the sea-level pressure field for ENSO warm events only. The anomalies in the areas of the Aleutian low (PNA) and the Iceland low (NAO) are of similar magnitude indicating the relative strength of the warm event response over the North Atlantic. Stratification with respect to very strong ENSO warm events (in terms of the sea surface temperature anomalies in the Indonesian area) reveals a dipole with positive sea level pressure anomalies over Scandinavia and the eastern parts of Europe and negative anomalies over western and central Europe; a weaker ENSO warm signal is dominated by a strong monopol-like negative anomaly over the North Atlantic/Central European region.

Kiladis and Diaz (1989, Figs. 2 and 3) composited the temperature and precipitation anomalies with respect to different stages of the life-cycle of the extreme ENSO warm and cold episodes. They basically substantiated the Van Loon and Madden (1981) results of the warm-cold event impact documenting an Aleutian monople associated with its opposing amplitudes and a dipole structure in the eastern North Atlantic/European sector with a meridional shift of the regional responses. The latter leads to the observed warm-cold composite fields over Europe indicating significant differences in the Scandinavian temperatures and the south-west European precipitation.

Halpert and Ropelewski (1992, Fig. 13) analysed ENSO warm and cold events to reveal the periods of largest ENSO-temperature response in various areas. They indicate "a potential ENSO/temperature relationship over northern Europe during the low (warm) phase and ENSO/temperature relationships during the high (cold) phase over western Europe/northern Africa and eastern Europe. The time series for the February to May season shows that 17 out of 20 cold event years had below normal temperatures". They also referred to Berlage (1966) who found some relationship between cold event relaxations and northwest European cold winters.

Given this background, the following discussion provides further qualitative evidence and quantitative details of a possible ENSO impact on Europe together with a physical diagnosis of the (upstream location and intensity of) dynamic sources associated with extreme anomalies in Europe. As these are closer to the tropical Pacific, they may represent the connection linking ENSO with European anomalies. The outline of the paper is as follows.

A phenomenological data analysis describes large scale circulation patterns (or Grosswetter) over Europe in terms of a binary point process responding on ENSO warm–cold episodes (Section 2).

A desriptive surface climatology of the possible ENSO induced European anomaly is provided by a statistical analysis of the sea level pressure field; the associated temperature and precipitation can be related to the shift of the sensitive tail end of the North Atlantic storm track (Section 3).

A physical data analysis is added for anomaly extremes observed in Europe (not neccessarily ENSO dependent): the related hemispheric 500 mb Eliassen-Palm flux diagnostics identifies transient and stationary eddy-mean flow interaction mechanisms and the associated upstream location and intensity of sources of wave activity (in the cyclogenesis area of the western North Atlantic) which may be affected at times by anomalies in the tropical Pacific (Section 4).

2. Weather regimes in the north Atlantic/European sector

The catalogue of 107 years of daily European weather types (from 1881 to 1987) consists of 29 classes characterizing sea level pressure over Europe and the eastern North Atlantic ("Grosswetterlage", see Hess and Brezowsky, 1977; and German Weather Service). They characterize centres of action during a time span of a few days corresponding to the passage of frontal systems. A dichotomous stochastic point process, $G(t)$ is defined to reduce the 29 weather types to a cyclonic ($C=1$) and an anti-cyclonic ($A=0$) regime over Europe (Fraedrich, 1990):

$$G(t) = C \text{ or } A,$$

i.e., $G(t)=1$ or 0. The number of cyclonic Grosswetter days, $N(i, j)$, for the $i=1, ..., 6$ bi-months and the $j=1, ..., J=107$ years is ranked from the smallest to the largest, $r(i, j)$, to obtain the order $N(i, 1)< \cdots < N(i, r)$. The percentile ranks, $R(i, j)=100r/J$ are then composited with respect to the warm and cold ENSO events.

2.1. *El Niño/Southern Oscillation events*

ENSO episodes cover an idealized (almost two year) period centered at the peak occurring at the end of the assigned ENSO year. The ENSO warm events are taken from Rasmussen and Carpenter (1983, Table 2; plus 1982 and 1986) covering 26 episodes; the ensemble of 21 cold events are taken from van Loon and Shea (1985, Table 1 plus 1975). The binary classification is composited in terms of percentile ranks evolving about the different stages of ENSO warm and cold episodes (Fig. 1). The following results represent warm and cold event ensemble averages of the percentile ranks.

The largest response is observed in the January/February bi-month at the peak of the event showing large and opposing deviations from the mean: a reduced (enhanced) number of cyclonic weather types in cold (warm) event winters. The reverse holds for the anticyclonic days.

Both signals decay at a similarly gradual rate but their growth is different. The warm event response appears to commence more abruptly in January/February, whereas the cold event counterpart evolves more gradually.

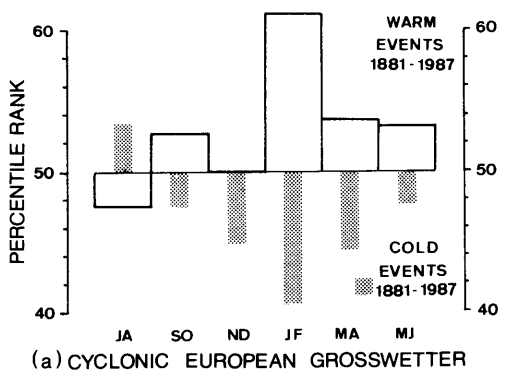

Fig. 1. Percentile ranks of the number of cyclonic European Grosswetter days composited about El Niño/Southern Oscillation warm and cold events based on 25 warm (open columns) and 21 cold (stippled columns) episodes.

A time series of J years has the percentile rank mean and variance, $\langle R(i, j)\rangle = 0.5 + 0.5J$ and $(1-1/J^2)/12$, tending towards 50% and $\pm 28.9\%$, respectively. That is, the warm–cold difference in winter is about a standard deviation, supporting the Wilcoxon (or Mann-Whitney) two-sided rank sum test, by which the null-hypothesis is rejected with 95% significance that warm and cold events have the same statistical population in common.

A complementary study (Wilby, 1993) with the Lamb (1972) catalogue of the daily weather types shows very similar effects of ENSO extremes on the synoptic climate of the British Isles. Even the daily synoptic records of both catalogues indicate the same results, namly that a response is most pronounced in the mid/end of February. Furthermore, both data analyses suggest that warm extremes are associated with highly variable winters; cold extremes tend to produce a more uniform response with less variation between individual events, and therefore they may have a higher predictability in long-range forecasting. Nontheless, this inherent variability severely limits the usefulness of ENSO for seasonal forecasting of weather patterns. 0ther phenomenological large scale circulation catalogues for the northern hemisphere mid- and higher latitudes also reveal an ENSO response (Fraedrich et al., 1992).

3. Surface climate anomalies in Europe

The European Grosswetter statistics is supplemented by the sea-level pressure (temperature and precipitation) anomaly response on both warm and cold ENSO event winters (December to February) based on 40 (43 and 36) stations in the 100-year interval (1888–1987; World Weather Records until 1970, Berliner Wetterkarte, 1971–1987). The climate mean is deduced from more than 80 years of simultaneous data, with 20 warm and 16 cold events. Significance has been estimated by a one-sided t-test (Fraedrich and Müller, 1992, Fig. 1).

The warm–cold composite sea level pressure difference is shown in Fig. 2. Warm episodes show a negative anomaly (<-1 mb) in central Europe with a zonal belt stretching from Ireland to the Black Sea and a positive anomaly (>1 mb) over northern and northeastern Europe (Scandinavia

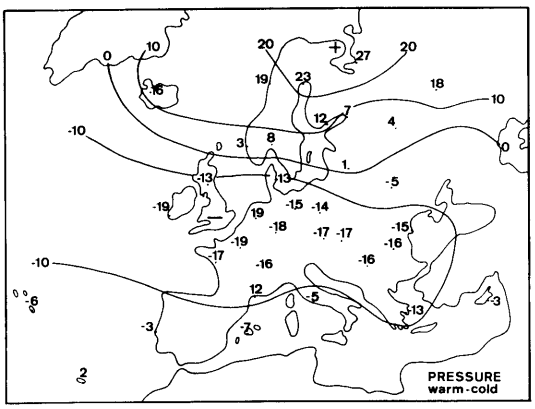

Fig. 2. Regional response in Europe on the El Niño/Southern Oscillation warm and cold extremes. Warm–cold difference of the DJF-mean sea level pressure (units in tenths of hPa) based on 40 stations (1887–1986).

and the Baltic states). The sign of the anomalies reverses during cold event winters; the strongest negative pressure anomalies (< -1 mb) are observed over Scandinavia, whereas the positive ones across the central and more southern parts of Europe are less intense. These composite pressure anomalies are in qualitative agreement with the European Grosswetter response showing enhanced cyclonic (anticyclonic) activity over Europe during warm (cold) events. Stations located at the core anomaly regions pass the 95% significance level (one in Scandinavia, four in Central Europe for warm and cold ENSO events).

3.1. *Temperature and precipitation*

The shift of the sensitive tail end of the North Atlantic storm track with its rainbearing frontal systems (documented by the surface pressure and Grosswetter anomalies over Europe, Figs. 1, 2) is associated with a response in the temperature and precipitation anomaly fields. Thus, as a direct consequence of this storm track shift, lower pressure, higher temperature and precipitation are observed over northern (and the reverse over central and southern) Europe in the cold event composite. The warm events show the opposite behaviour (see, for example, Fraedrich and Müller, 1992; Figs. 1, 2). Ropelewski and Halpert (1987, 1989; analysing only warm episodes associated with highly variable winters) did not mention the precipitation response in Europe to be of particular relevance (see, however, Kiladis and Diaz (1989), analysing the warm–cold differences; Fig. 3).

3.2. *General circulation model (GCM) experiments*

For the recent warm and cold ENSO episodes, 120-day ensemble integrations from the T63 ECMWF model (Palmer and Anderson, 1994; Brankovic et al., 1994) were started on 9 consecutive days (1–9 November). The first ensemble integration was initialized using data from 1986 and integrated with global observed sea surface temperatures (SSTs) from the warm ENSO winter 1986/87. The second ensemble was initialized using data from 1988, and integrated with observed SSTs of the cold ENSO winter 1988/89. Fig. 3 show the ensemble mean 1000 mb height difference 1986/86–1988/89 of the ensemble integrations and the operational analyses to be in general agreement. "Over the Atlantic and Europe, the pattern of height difference is well simulated though the magnitude of the difference field is clearly too weak, associated with considerable variability within the ensemble." This is consistent with the observational studies that there is an impact of El Niño over Europe, though it is not large compared with the magnitude of the internal variability. Indeed, the observed ENSO composites (Fig. 2) compare well with the difference field in Fig. 3b (Palmer and Anderson, 1993, Fig. 5). Furthermore, the variability amongst the ensemble members in the NWP-experiment corresponds to the natural variability in the warm and cold ENSO-events (Fraedrich and Müller, 1992).

The observed circulation anomalies in the North Atlantic/European sector appear to be also correlated with mid-latitude SST anomalies near Newfoundland (in the cyclogenesis area of the North Antlantic storm track), which can have an influence on the downstream atmospheric development (Palmer and Sun, 1985; Rowntree, 1976). This explains why a downstream tracing of a possible ENSO-response over Europe is blurred by such "noise effects". However, these processes may not necessarily be stochastic, but nonlinear. Therefore, in the next step, we try to identify possible sources affecting European climate anomalies (which are, for example associated with upstream sources of wave activity) that could be linked to the ENSO signal and influence Europe by downstream propagation.

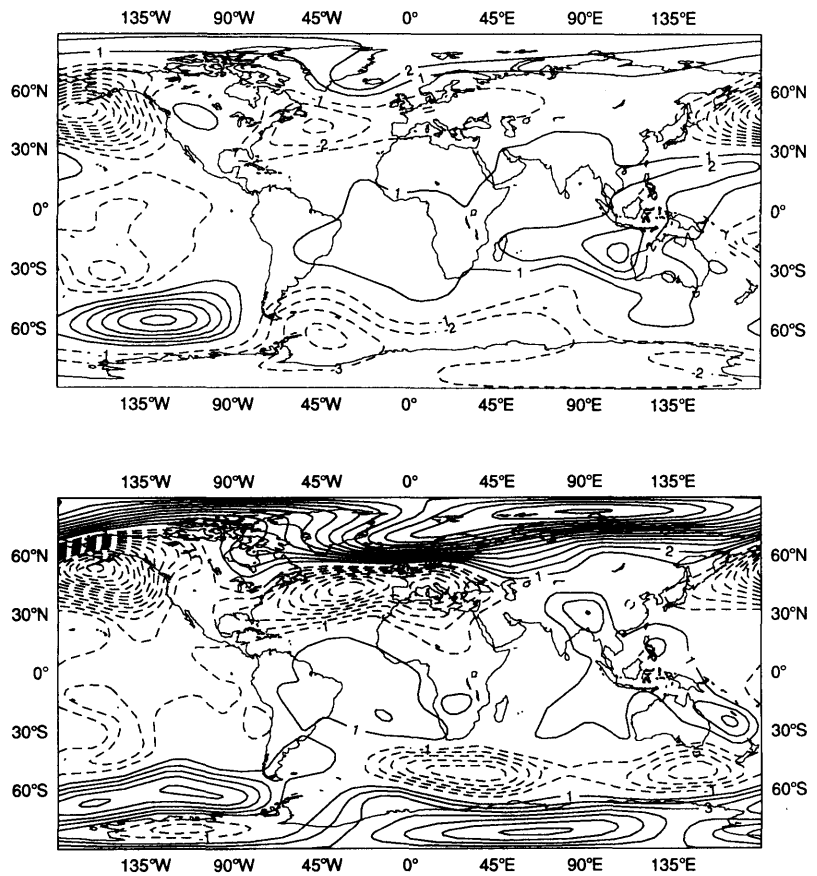

Fig. 3. Seasonal mean 1000 mb height difference estimates for DJF 1986/7 minus DJF 1988/9: (a) The 9 member ensemble mean integrations initiated on 1, ..., 9 November and run with observed SSTs, (b) the operational analyses. Contour interval 1 dam (from Palmer and Anderson, 1993).

4. Transient and stationary eddy-mean flow interaction

The following diagnostic analysis of extreme European winter climate anomalies has two goals: the identification of the spatial structure and the association with the upstream location and intensity of sources of transient and stationary wave activity (Fraedrich et al., 1993). These source regions may, under favourable conditions, be the cutting edge for a possible ENSO-Europe connection. This diagnostics has been chosen, because possible dynamical ENSO-Europe links are likely to be strongly influenced by external processes, like the North Atlantic oscillation etc. and nonlinear interactions, which cannot be extracted by correlation type analyses. If there is any hope to identify mechanisms, they should become evident in the strongest possible anomalies observed over Europe. Therefore, this section is included to estimate upstream *dynamic* associations of these anomalies, i.e., given a response or climate anomaly in Europe (which is not necessarily connected with ENSO), how far can this signal be traced upstream to its origin by applying dynamical methods which are not confined to the standard zonally averaged information. The upstream location and intensity of the source may then be (nonlinearly) linked to ENSO related dynamical processes. This procedure is followed,

because direct ENSO-Europe correlations did not show very satisfactory results when using fields of higher moments (eddy fluxes) based on daily data.

4.1. *Anomaly patterns*

European climate anomaly patterns of individual winter months (December, January and February, DJF, 1887–1986) are constructed by a simultaneous empirical orthogonal function (EOF) analysis of the sea level pressure, temperature and precipitation at 40 European stations, which are selected to give an optimally homogeneous distribution over Europe (World Weather record until 1970 and Berliner Wetterkarte from 1971). The first and the second eigenvector of the simultaneous dataset represent about 45% of the total variance. The first EOF of the pressure field alone describes about 45% and the loading of the second one reduces to almost 25%. The spatial pressure field patterns of both first EOFs (pressure alone and simultaneous) are very similar, their amplitudes are highly correlated explaining more than 80% of each others variance, and there is almost no change of their structure notable after rotation of the eigenvectors.

The *spatial structure* of the first EOF is characterized by a high (low) pressure cell over central Europe. The associated positive (negative) temperature and precipitation anomaly over northern (central–southern) Europe is indicative of a northward (southward) shift of the tail end of the cross-Atlantic storm track. These patterns resemble the phenomenological anticyclonic (cyclonic) Grosswetter or the European blocking (enhanced zonal flow) regime.

The *time structure* of the first EOF amplitudes (principle components, E1) and their frequency distribution reveals bimodality (Table 1). It appears that the simultaneous treatment of the three variables characterizing the European climate shows regional climate state bimodality. This observed bimodality provides some additional support for the bimodal probability density distribution observed in the general circulation in the wavenumber 2 to 4 amplitudes of NMC analyses of 16 winter seasons (for example, Hansen and Sutera, 1986).

Table 1. *Frequency of 300 monthly amplitudes, E1, of the first simultaneous pressure-temperature-precipitation European climate eigenvector (Fraedrich et al., 1993)*

E1:	−25	−20	−15	−10	−5	0	5	10	15	20	25	30
freq:	2	8	17	26	**52**	45	41	**45**	40	17	6	1

All this suggests that the amplitude E1 of the first simultaneous EOF (comprising the 3 European climate anomaly state variables) appears to be a useful index characterizing the climate anomaly state in winter months. The observed bimodality is not a neccesary requirement but supportive. Due to the apparent qualitative similarities between the ENSO response mode (Fig. 3) and the first simultaneous EOF (Fig. 4a), we extend the diagnostics to the daily hemispheric 500 mb geopotential height fields (NCAR, $5° \times 5°$ grid, north of 20°N, 1946–87, obtained from MPI für Meteorologie, Hamburg) to identify location and intensity of upstream sources of wave activity. Although associated with extreme winter anomalies in Europe these source regions may possibly be affected at times by signals propagating out of the tropical Pacific.

4.2. *Eddy and mean flow fields*

The hemispheric daily geopotential height fields comprise 41x3 winter months of which both the original and a band-pass filtered (Blackmon and Lau, 1980; 21-point filter retaining the 2.5 to 6 day band) data set are analysed. The fields are composited about the following ten winter months with an extreme positive and negative E1-index: (a) High pressure ($E1 > 0$): F59, J64, D53, D63, D72, F56, D71, F75, F49, D48 and (b) low pressure ($E1 < 0$): J48, D65, F77, F66, D81, F57, J84, F55, F70, D79. The flow fields are subjected to further analysis: monthly mean geopotential heights, Z, to deduce the stationary wave activity flux from the zonally asymmetric circulation, Z^*, and the monthly variances of the band-pass filtered geopotential height and geostrophic wind components $\langle Z'^2 \rangle$, $\langle u'^2 \rangle$, $\langle v^{2\prime} \rangle$ and the covariance $\langle u'v' \rangle$ to deduce the transient wave activity flux. The eddy statistic represents departures from the means of each individual month.

Fig. 5 shows the high and low E1-composites (related to high and low sea level pressure anomalies over Europe, respectively) of the hemispheric band-pass filtered geopotential height variances (top) and the stationary geopotential height anomalies (bottom).

High (low) pressure anomalies over Europe are

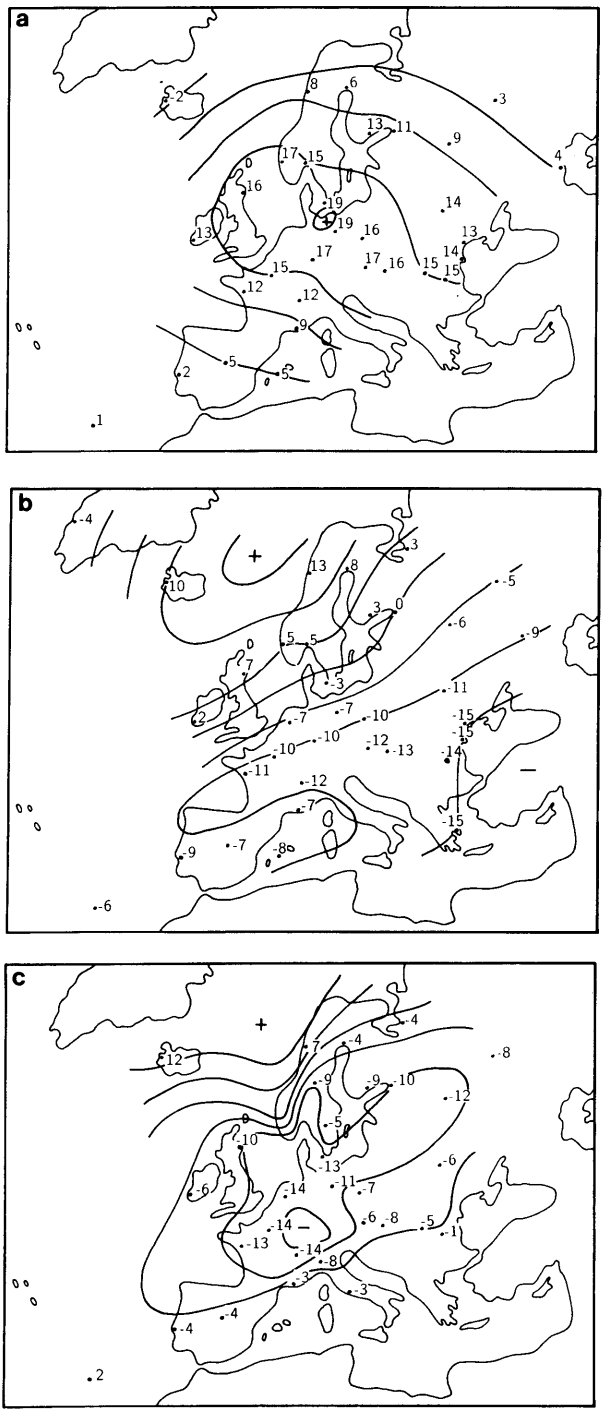

Fig. 4. The geographical distribution of (a) monthly mean sea level pressure, (b) temperature and (c) precipitation over Europe (1887–1986): the first eigenvector.

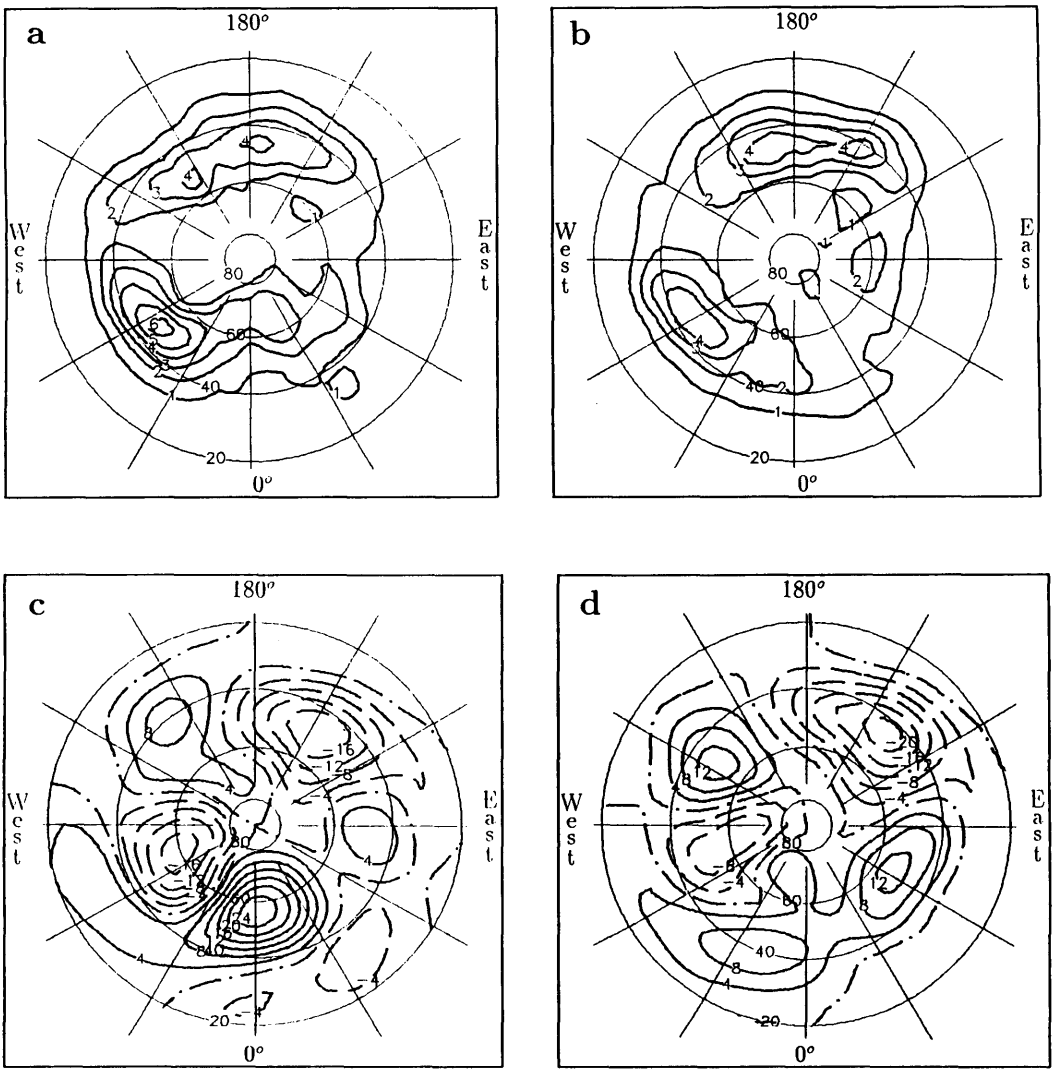

Fig. 5. Transient (band-pass filtered) eddy variance of the daily hemispheric 500 mb geopotential height (top: a and b) and the stationary geopotential height anomaly (bottom: c and d) for extreme winter months in Europe: high and low pressure composites.

associated with enhanced (reduced) transient activity of the band-pass filtered eddies in the region of cyclogenesis in the western North Atlantic; there is a stronger (almost normal) jet maximum over the east coast of North America and the eddies follow the northward (zonal) route of the tail end of the cross Atlantic storm track. Near the tail end of the Pacific storm track the composites reveal an interesting feature: during high pressure situations in Europe (i.e., blocking or reduced zonal flow) the strongest activity of the transient eddies over the North Pacific extends about 10–20° longitude further eastward/southeastward and closer to the west coast of North America. The associted transient wave activity fluxes in terms of the extended Eliassen-Palm flux provide more information (see below).

The positive or high pressure composite shows a

strong western North Atlantic source of stationary wave activity due to an intense cross-Atlantic Z^*-dipole. The reverse holds for the negative or low pressure composite when the deviations, Z^*, from the zonal mean are very weak. Note that the climate mean over Europe has a strong positive deviation. More details are obtained from the stationary wave activity fluxes associated with wave train propagation.

4.3. *Transient eddy-mean flow forcing*

The extended Eliassen-Palm flux diagnostics is introduced to obtain a dynamic interpretation of the transient eddy-mean flow interaction. The extended Eliassen-Palm flux or E-vector has been described by Hoskins et al. (1983):

$$\boldsymbol{E} = -\{\langle u'^2\rangle - \langle v^{2\prime}\rangle; \langle u'v'\rangle\}.$$

With the assumption that the zonal scale of the transient eddies is much larger than the meridional scale, the E-vector can be related to the barotropic conversion of energy from the transient eddies to the time mean flow, C, the forcing, S, of the mean stream function, and the eddy forcing of the mean flow, F (see also Wallace and Lau, 1985):

$$C = -\boldsymbol{E}\cdot\operatorname{grad} U,$$

$$S = -\operatorname{grad}^{-2}\{\operatorname{div}\langle v'\zeta'\rangle\},$$

$$F = -S_y = \operatorname{grad}^{-2}\{\operatorname{div}\langle v'\zeta'\rangle\}_y.$$

The last two terms are conveniently approximated by $S = -\operatorname{grad}^{-2}\operatorname{div}\boldsymbol{E}_y$, $F = -S_y = \operatorname{div}\boldsymbol{E}$; U is the mean geostrophic wind component and ζ the geostrophic vorticity. The forcing, F, of the time mean flow by the band-pass filtered transient eddies is consistent with the tendency to increase the westerly mean flow. At the centres of eddy activity, where $\langle u'v'\rangle_y > 0$, eddy momentum transports tend to accelerate the westerly mean flow north of the jet axis; poleward and further south of a zonally oriented storm track axis there are poleward or equatorward accelerations affecting the meridional flow, because $-\{\langle u'^2\rangle - \langle v'^2\rangle\}_y > 0$ or <0, respectively. The mean stream function forcing, S, may be analysed to reduce small scale noise and to locate sources and sinks of the mean stream function due to transient eddy activity. Note that the group velocity of the transient perturbations relative to the time mean flow has twice the angle of the E-vector to the x-axis, provided the mean absolute vorticity gradient is meridional. The high and low pressure anomaly composites of the E-vector are shown in Fig. 6a, b.

The E-vector field of the high pressure composite (E1 >0) shows relatively large intensities and an almost continuous stream of eastward directed E-vector bundles extending from the western North Pacific to the central North Atlantic (near 30° W). The northward bifurcation in the North Atlantic coincides with the observed storm track shift. The E-vectors show a strong convergence in the region about 55° N; 0° E, which is associated with an easterly forcing of the mean flow. In northern Europe (where div $\boldsymbol{E} > 0$) transient eddies generate westerly momentum through eddy-mean flow interaction supporting/enhancing the mean anticyclonic vorticity and the high pressure anomaly over Europe (once initially established, see below).

The low pressure anomaly composite is confined to a basically zonal E-vector flow in the North Atlantic basin without a northward shift nor a prolongation of the storm track.

4.4. *Stationary wave propagation*

For quasi-geostrophic waves on a zonal flow a locally applicable conservation equation has been derived to provide a diagnostics of the propagation of stationary wave activity. Applications (see, for example, Karoly et al., 1989) are confined to the horizontal components, $\boldsymbol{F} = \{F_x, F_y\}$, of the originally three-dimensional stationary wave activity flux (Plumb, 1985, eq. 4.9):

$$\boldsymbol{F} = \{F_x, F_y\}$$
$$= (s/2f^2)\{Z_y^{*2} - Z^*Z^*_{xx}; Z^*_xZ^*_y - Z^*Z^*_{xy}\},$$

where $s = p/1000$ hPa. The F-vector has been computed from the zonally asymmetric part of the time (monthly) mean geopotential, Z^*, and mapped onto polar stereographic coordinates. The wave activity flux is presented in Fig. 6 (c, d) as in Plumb (1985).

Extreme high pressure anomalies in Europe are associted with an intense stationary wavetrain, which emanates from the region of western Atlantic cyclogenesis and propagates across the North Atlantic dissolving over the eastern Atlantic/European sector. The stationary wavetrain does not exist in the European low pressure composite.

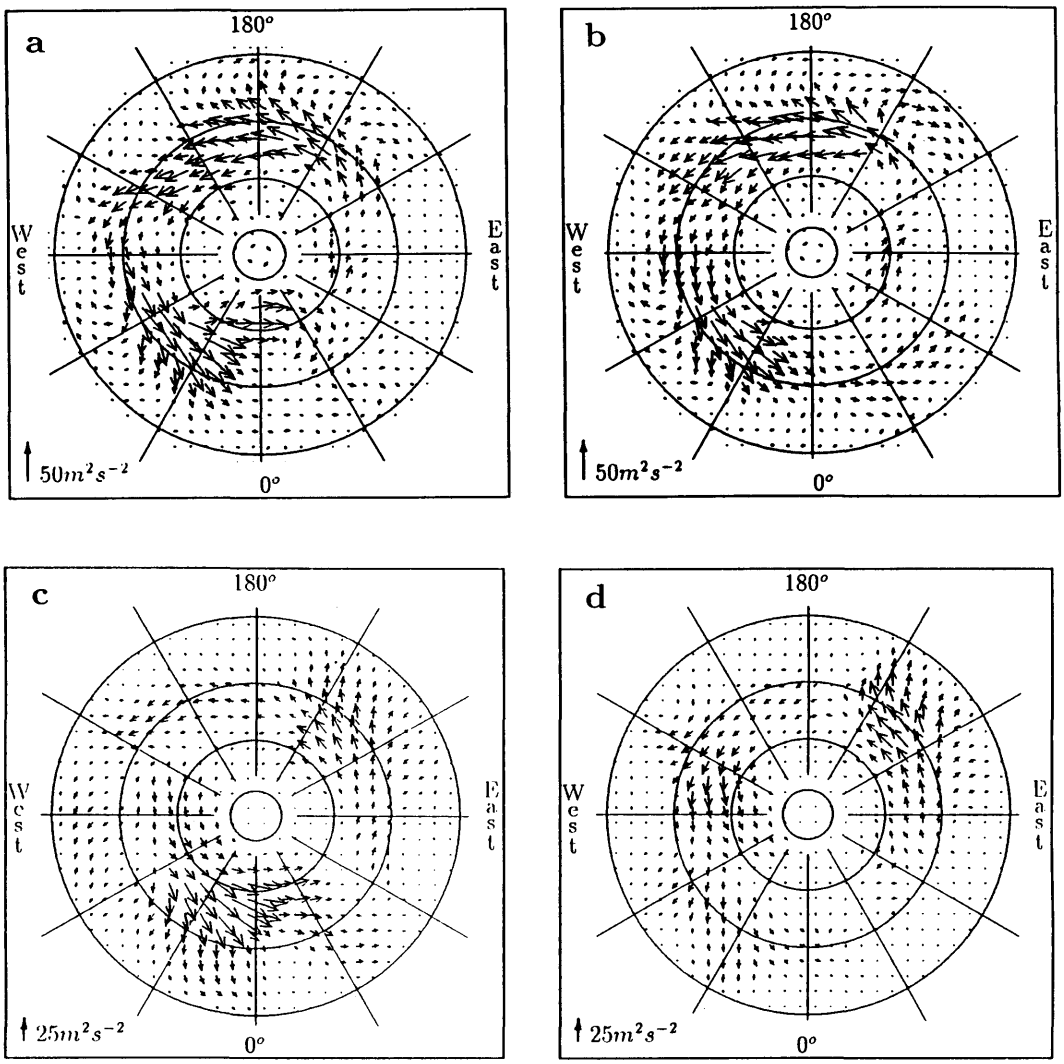

Fig. 6. Extended Eliassen-Palm flux of transient wave activity (top: a and b) and stationary wave activity flux (bottom: c and d) associated with the band-pass filtered transient eddy variance and stationary anomalies (see Fig. 5) for extreme winter months in Europe: high and low pressure composites.

This Rossby wave train, although observed simultaneously with the European climate anomaly, may serve as the missing mechanism generating an initially small, high pressure perturbation, which shifts the sensitive tail end of the North Atlantic storm track northward. The subsequent transient eddy-mean flow interaction may then enhance this initially small perturbation to a persistent high pressure anomaly over Europe.

The physical diagnostics discussed in this section has been introduced to supplement the phenomenological (Section 2) and statistical (Section 3) analyses of a possible ENSO impact on European climate anomalies. This analysis of wave activity has been chosen to trace the source regions of propagating transient and stationary waves (associated with European anomaly extremes) as far upstream as possible. It appears neccesary to

analyse both transient and stationary eddy activity fluxes, because the stationary wave train may provide the initial perturbation (modifying the sensitive storm track tail) which the transient eddy-mean flow interaction may turn into a persistent anomaly over Europe. In contrast to the sensitive tail end of the North Atlantic storm track (or region of cyclolysis) the location of the cyclogenesis area (in the western North Atlantic) is resilient to perturbations, but not their intensity or transient eddy source strength. That is, the cyclogenesis area may be a focal point for the possible ENSO-Europe link observed at times. It may be influenced by signals propagating downstream from the tropical and northern parts of the Pacific.

5. Conclusion and discussion

In this paper, we attempt a synthesis of a set of data analyses on possible ENSO-Europe connections which, though observed at times, are neither very well understood nor, for many scientists, convincingly demonstrated. This is plausible because long-distance transmissions of meteorological signals are modified by external fluctuations, in particular in the mid-latitudes, where the "noise level" may almost completely hide atmospheric teleconnections. Therefore, only under favourable situations (demonstrated in Section 3) and using conditional statistics, one may hope to gain more insight into the physical mechanisms leading to very long distance teleconnections, such as the possible ENSO-Europe link. A conditional statistics needs to be applied both to the forcing (that is, the ENSO warm or cold event) and to the response (that is, the European climate anomaly). The first analysis (in terms of a neccesary condition, Sections 1–3) gave some support for an ENSO-Europe connection using the phenomenological and climate statistics approach, together with GCM-experiments. This conclusion may not be reached when using unconditional (linear) correlation techniques based on sea surface temperature fields etc. as predictor (Barnston, 1993), because the response modes of the North-Atlantic storm track can be asymmetric in position, phase and intensity. The second approach (in terms of a sufficient condition, Section 4) is more physically oriented. Here an attempt is made to identify location and intensity of the sources of transient and stationary wave activity which are associated with extreme anomalies in Europe (not neccesarily related to ENSO). The aim was to trace optimally large (response) signals over Europe as far upstream as possible before they are covered in the "noise" of other atmospheric fluctuations. These source regions associated with the mechanisms of wave propagation/mean flow interaction (which form the basis of the analysis techniques) may be the link, connecting ENSO forcing in the tropical Pacific with a possible far distant European response. Finally, it should be stressed that these conjectures are highly speculative and other interpretations of the data are conceivable. This will be subject of further research.

6. Acknowledgements

This paper is based on a lecture at the Workshop on short-term climate prediction (April 1993) held at the Max Planck Institut für Meteorologie, Hamburg, and invited lectures at the European Geophysical Society (EGS) Meeting (May 1993) in Wiesbaden, and at the Workshop on the "Scientific assessment of the prospect of seasonal forecasting: a European perspective" (December 1992) at the European Centre for Medium Range Weather Forecasts (ECMWF) in Reading. The discussions and comments at these meetings, with Kingtse Mo, CAC, and the supply of Fig. 5 by Tim Palmer are gratefully acknowledged.

REFERENCES

Barnston, A. G. 1994. Linear statistical short-term climate predictive skill in the northern hemisphere. Part 1: Cold season results, Part II: Non-cold season results. *J. Climate* 7, in press.

Berlage, H. P. 1966. *The Southern Oscillation and world weather*. K. Ned. Meteorol. Inst. Meded. Verh., 88, 152 pp.

Blackmon, M. L. and Lau, N.-C. 1980. Regional charac-

teristics of the northern hemisphere winter time circulation. A comparison of a GFDL general circulation model with observations. *J. Atmos. Sci.* **37**, 497–514.

Brankovic, C., Palmer, T. N. and Ferranti, L. 1994. Predictability of seasonal atmospheric variations. *J. Climate* **7**, 217–237.

Fraedrich, K. 1990. European Grosswetter during the warm and cold extremes of the El Niño/Southern Oscillation. Intern. *J. Climatol.* **10**, 21–31.

Fraedrich, K. and Müller, K. 1992. Climate anomalies in Europe associated with ENSO extremes. Intern. *J. Climatol.* **12**, 25–31.

Fraedrich, K., Bantzer, C. and Burckhardt, U. 1993. Winter climate anomalies in Europe and their associated circulation at 500 hPa. *Climate Dynamics* **8**, 161–175.

Fraedrich, K. K. Müller and Kuglin, R. 1992. Northern hemisphere circulation regimes during the extremes of the El Niño/Southern Oscillation. *Tellus* **44A**, 33–40.

Halpert, M. S. and Ropelewski, C. F. 1992. Surface temperature patterns associated with the Southern Oscillation. *J. Climate* **5**, 577–593.

Hamilton, K. J988. A detailed examination of the extratropical response to tropical El Niño/Southern Oscillation events. *J. Climatol.* **8**, 67–86.

Hansen, A. R. and Sutera, A. 1986. On the probability distribution of planetary scale atmospheric wave amplitude. *J. Atmos. Sci.* **43**, 3250–3265.

Hess, P. and Brezowsky, H. 1977. *Katalog der Grosswetterlagen.* Ber. Dtsch. Wetterdienst, Offenbach, 113, Bd. 15, 39 pp.

Hoskins, B. J., James, I. N. and White, G. H. 1983. The shape, propagation and mean-flow interaction of large scale weather systems. *J. Atmos. Sci.* **40**, 1595–1612.

Karoly, D. J., Plumb, R. A. and Ting, M. 1989. Examples of the horizontal propagation of quasi-stationary waves. *J. Atmos. Sci.* **46**, 2802–2811.

Kiladis, G. N. and Diaz, H. F. 1989. Global climatic anomalies associated with extremes in the Southern Oscillation. *J. Climate* **2**, 1069–1090.

Lamb, H. H. 1972. British Isles weather types and a register of the daily sequence of circulation patterns, 1861–1971. *Geophys. Mem. no. 116*, HMSO, London, 85 pp.

Palmer, T. N. and Anderson, D. L. T. 1993. *Scientific assessment of the prospect of seasonal forecasting: a European perspective.* European Centre for Medium-Range Weather Forecasts. Technical Report, 70, 34 pp.

Palmer, T. N. and Anderson, D. L. T. 1994. The prospects for seasonal forecasting. *Quart. J. R. Meteorol. Soc.* **120**, in press.

Palmer, T. N. and Sun, 1985. A modelling and observational study of the relationship between sea surface temperature anomalies in the north–west Atlantic and the atmospheric general circulation. *Quart. J. R. Meteorol. Soc.* **111**, 947–975.

Plumb, R. A. 1985. On the three-dimensional propagation of stationary waves. *J. Atmos. Sci.* **42**, 217–229.

Rasmussen, E. M. and Carpenter, T. H. 1983. The relationship between eastern equatorial Pacific sea surface temperatures and rainfall over India and Sri Lanka. *Mon. Wea. Rev.* **111**, 517–528.

Ropelewski, E. M. and Halpert, M. S. 1987. Global and regional precipitation patterns associated with the El Niño/Southern Oscillation. *Mon. Wea. Rev.* **115**, 1606–1626.

Ropelewski, E. M. and Halpert, M. S. 1989. Precipitation patterns associated with the high index phase of the Southern Oscillation. *J. Climate* **2**, 268–284.

Rowntree, P. R. 1976. Response of the atmosphere to a tropical Atlantic Ocean temperature anomaly. *Quart. J. R. Meteorol. Soc.* **102**, 607–625.

Van Loon, H. and Madden, R. A. 1981. The Southern Oscillation, Part I. Global associations with pressure and temperatures in northern winter. *Mon. Wea. Rev.* **109**, 1150–1162.

Van Loon, H. and Shea, D. J. 1985. The Southern Oscillation, Part IV. The precursors south of 15°S to the extremes of the oscillation. *Mon. Wea. Rev.* **113**, 2063–2074.

Wallace, J. M. and Lau, N.-C. 1985. On the role of barotropic energy conversions in the general circulation. *Adv. Geophys.* **28A**, 33–74.

Wilby, R. 1993. Evidence of ENSO in the synoptic climate of the British Isles since 1880. *Weather* **48**, 234–239.

Printed in Belgium